Hindawi
International Journal of Antennas and Propagation
Volume 2021, Article ID 4657540, 8 pages
https://doi.org/10.1155/2021/4657540

*Research Article*

# A Dual-Band Base Station Antenna with a Split Ring for Sub-6 GHz Communication

**Bei Huang**,[1,2] **Jie Cao**,[3] **Weifeng Lin**,[3] **Jun Zhang**,[3] **Gary Zhang**,[3] **and Fugen Wu**[1]

[1]*School of Materials and Energy, Guangdong University of Technology, Guangzhou 510006, China*
[2]*School of Electronics and Information, Guangdong Polytechnic Normal University, Guangzhou 510665, China*
[3]*School of Information Engineering, Guangdong University of Technology, Guangzhou 510006, China*

Correspondence should be addressed to Jun Zhang; junzhang@gdut.edu.cn

Received 26 June 2021; Revised 15 August 2021; Accepted 31 August 2021; Published 9 September 2021

Academic Editor: Paolo Burghignoli



A dual-band base station antenna is introduced in this paper. The proposed antenna is composed of baluns, bowtie patches, and a split ring. The two pairs of bowtie patches excited by the two orthogonal balun structures can achieve dual polarization. The split ring is used to yield two additional resonances to broaden the impedance bandwidth. In this way, a compact dual-band base station antenna is obtained with the size of $0.41\ \lambda_c \times 0.41\ \lambda_c \times 0.13\ \lambda_c$ ($\lambda_c$ is the wavelength in the free space at the lowest operating frequency band) and the average gain of 8.2 dBi. Moreover, the operating frequency bands of the proposed antenna cover 2515–2675 MHz, 3400–3600 MHz, and 4800–5000 MHz, which can function as an element for macro- or microcells in sub-6 GHz communications.

## 1. Introduction

Because of the rapid development of mobile communication, the demands for high-speed and low-latency data services are enormously increasing [1]. It is considered that the sub-6 GHz band ranging from 2 to 6 GHz serves as the primary frequency band in the early era of the fifth generation (5G), providing an optimal balance between coverage and capacity. The frequency bands of N41 (2515–2675 MHz), N78 (3400–3600 MHz), and N79 (4800–5000 MHz), divided by the Third Generation Partnership Project (3GPP), are specified for sub-6 GHz communication. To obtain ubiquitous access in indoor scenarios, microbase stations need to be densely deployed. Therefore, dual-band base station antennas with compact size and low cost are highly in demand.

As we know, the microstrip antenna has merits of low profile, easy fabrication, and low cost, but a narrow impedance bandwidth [2]. By loading parasitic elements [3, 4], another resonance occurs near the main resonant frequency. A parasitic loop is placed below the two crossed dipoles and a parasitic disk, so that the bandwidth in [5] is also enhanced. A hybrid-mode antenna is a promising candidate to broaden the bandwidth through sequentially exciting several modes in a shared aperture structure [6]. A dual-wideband dual-polarized aperture-shared patch antenna with high isolation was presented in [7], which is composed of an X-band linearly polarized antenna and S-band circularly polarized antenna. The stacked patches are applied in the S-band antenna, where the upper parasitic patch is used to increase the gain and bandwidth and also works as a ground plane for the X-band exciting patch. The X-band feed coaxial line perforates the center of the parasitic patch and S-band excited patch so that the shared aperture antennas are tightly integrated with high isolation. However, the complexity of this antenna may be not suitable for base-station applications.

By utilizing a pair of ring dipoles and Y-shaped feeding lines, a broadband dual-polarized antenna for LTE/5G base applications was presented in [8]. When one ring dipole is excited, the other is regarded as the parasitic element to

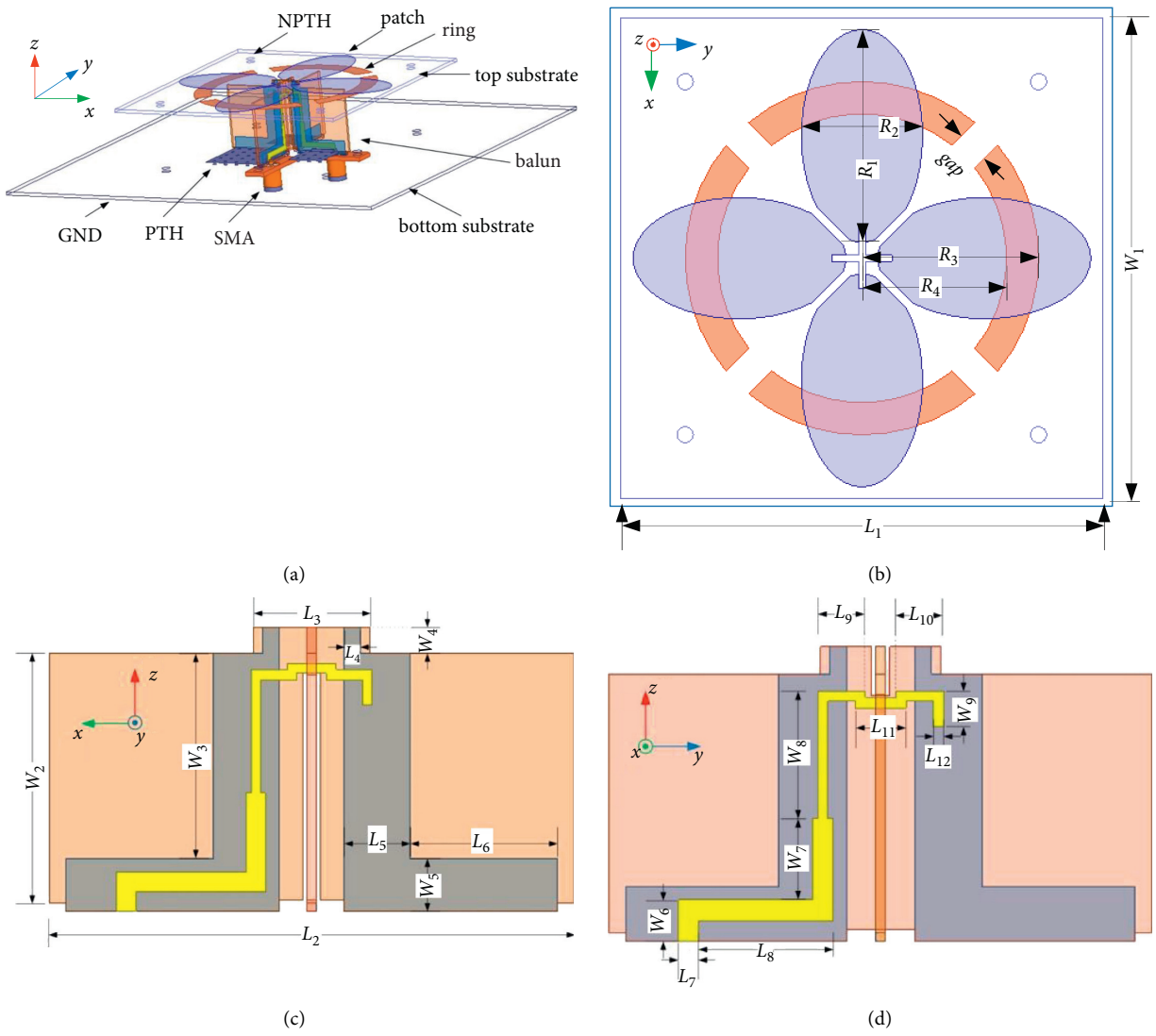


FIGURE 1: Geometry of the proposed antenna. (a) Perspective view, (b) the major radiator (two pairs of bowtie patches and an SR), (c) the balun structure in the *xoz* plane, and (d) the balun structure in the *yoz* plane.

broaden the bandwidth effectively. It achieves a wide band of 48.6% from 2.21 to 3.63 GHz with a stable gain of 8.3 dBi. Also, a compact dual-band dual-polarized base station was proposed in [9]. The dual-band performance is achieved by integrating a small oval-shaped loop within the large oval-shaped loop without increasing the size of the radiating patch. It covers the frequency bands from 3.3 to 3.8 GHz and 4.8 to 5.0 GHz. However, these antennas either cover the low-mid frequency band or mid-high frequency band within sub-6 GHz.

In this paper, two pairs of bowtie patches and a split ring (SR) are shared in a common aperture. The SR is regarded as a parasitic patch to broaden the impedance bandwidth. A dual-band base station antenna is achieved for sub-6 GHz communication, which covers the frequency bands of N41 (2515–2675 MHz), N78 (3400–3600 MHz), and N79 (4800–5000 MHz).

## 2. Antenna Design and Analysis

*2.1. Antenna Structure.* The geometry of the proposed antenna is presented in Figure 1. The antenna consists of four parts: top substrate, bottom substrate, and two balun structures. The substrates used are the low-cost FR4 material with a relative permittivity of 4.40 and a loss tangent of 0.02. The thickness of both top and bottom substrates is 0.80 mm, while that of the balun substrate is 0.60 mm. The rest dimensions of the presented antenna are detailed in Table 1.

Two pairs of orthogonal bowtie patches are printed on the upper side of the top substrate. This setup is to ease the assembly and soldering process since the bowtie patches are electrically connected with the balun structures. The SR is placed on the lower surface of the top substrate, improving the matching and radiation performance through the introduction of additional resonances. Moreover, to make the

Table 1: Dimensions of the proposed antenna.

| Parameter | Value (mm) |
|---|---|
| $R_1$ | 26.5 |
| $R_4$ | 18.0 |
| $L_2$ | 32.0 |
| $L_5$ | 4.0 |
| $L_8$ | 7.9 |
| $L_{11}$ | 3.0 |
| $W_2$ | 15.2 |
| $W_5$ | 3.2 |
| $W_8$ | 7.5 |
| $R_2$ | 15.6 |
| gap | 4.0 |
| $L_3$ | 7.1 |
| $L_6$ | 9.0 |
| $L_9$ | 2.2 |
| $L_{12}$ | 0.6 |
| $W_3$ | 12.5 |
| $W_6$ | 2.5 |
| $W_9$ | 1.0 |
| $R_3$ | 22.0 |
| $L_1$ | 60.0 |
| $L_4$ | 1.0 |
| $L_7$ | 1.2 |
| $L_{10}$ | 2.2 |
| $W_1$ | 60.0 |
| $W_4$ | 1.6 |
| $W_7$ | 4.8 |

two ports as symmetrical as possible, the microstrip feeding line of the balun near the upper substrate is convex in the *xoz* plane and concave in the *yoz* plane. Also, the amplitude of the bump and depression is the same, as shown in Figures 1(c) and 1(d). In addition, the balun also plays the role of impedance transformer.

*2.2. Operating Principle.* To understand the operating principle of the proposed antenna, the evolution of the proposed antenna is shown in Figure 2. The occurrence of the adjacent resonances can effectively widen the impedance bandwidth once the inductance and capacitance of the two modes compensate for each other [2–5]. It can be noted that the structure in Figure 2(b) has one more SR compared with Figure 2(a), which is the same as the structure in Figure 2(d) compared with Figure 2(c). Meanwhile, the structure in Figure 2(c) has one more balun structure compared with Figure 2(a), which is the same as the structure in Figure 2(d) compared with Figure 2(b). Together with the three reference antennas, the structure evolution is helpful to demonstrate the functionality of the SR and the balun. The inductance component is provided with the ring itself, while the capacitance one is located at the split ends [10]. Additional resonances are excited by the SR, where the bandwidth could be expanded through the presence of the adjacent resonances.

Figure 3 presents the input impedance of the proposed and reference antennas. There is only one resonance when only the bowtie patch functions. At the presence of SR, two additional resonances occur. We can see that the third and fifth resonances of the proposed antenna are determined by the SR. Comparing Ref. 1 with Ref. 3 or Ref. 2 with the proposed antenna, we can find that the balun structure is used not only to transform the impedance and match the 50 Ω SMA but also to generate additional resonances to increase the impedance bandwidth. Compared to a whole ring patch, the SR has less stored energy and thus a lower Q-factor [11] which implies a wider bandwidth for the proposed antenna.

Figure 4 displays the simulated current distributions on the bowtie patches and SR at different frequencies. The currents of the SR and the bowtie patches are in the opposite direction, which is of benefit to reducing stored energy near the antenna volume [12]. The current near the center of the bowtie patches is spread due to the presence of the parasitic SR. To further illustrate the role of the SR, the comparison with and without the SR is conducted in Figure 5. There is around 1-dBi increase on the gains with the SR because of the improvement in both the matching and radiation performance by introduction of the third and fifth resonances. It is noted that there is a gain drop near 4.0 GHz because of the generation of the trapped mode; however, it has little effect on the operating band of this antenna.

## 3. Results and Discussion

To verify this design, a prototype of the presented antenna has been fabricated and tested, as shown in Figure 6. Nylon screws are applied to support the frame. The reflection coefficient was measured by using a Keysight E5071C vector network analyzer, whereas the gain and radiation patterns were measured by using a Satimo StarLab system, ranging up to 5.80 GHz.

Figures 7 and 8 illustrate the measured S parameters and peak realized gains of the proposed antenna, respectively. The measured impedance bandwidth ranges from 2.30 to 3.70 GHz and 4.70 to 5.90 GHz, where the frequency bands of N41, N78, and N79 are covered. The measured mutual coupling between the two ports is lower than −23 dB. The radiation patterns of the proposed antenna in the *xoz* plane and the *yoz* plane are displayed in Figure 9. The measured results are consistent with the simulated ones.

A comparison between the proposed antenna and previous dual-band base station antennas is presented in Table 2. Two crossed dipoles are used to realize the dual polarization in [14], and the structure is sturdy, but the impedance bandwidth is low. The structure of the antenna in [17] is simple, and it could cover the WLAN 2.4-GHz (2.40–2.48 GHz) and 5-GHz (5.15–5.85 GHz) with isolation >27 dB. The profile in [18] is low, but the size is a little large. Compared with [18, 19], the proposed antenna could cover the most frequency bands for sub-6 GHz communications. For the simulated radiation efficiency in the operating band, the minimum value is 91.62% at 3.60 GHz while the maximum value is 95.19% at 3.40 GHz, which exhibits the advantage of the proposed antenna because of the lossy substrate [20, 21].

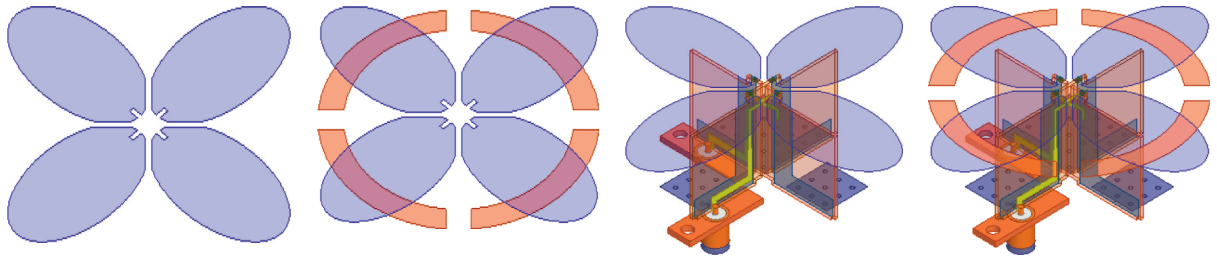


Figure 2: Evolution of the proposed antenna. (a) Ref. 1: patch + GND. (b) Ref. 2: patch + SR + GND. (c) Ref. 3: patch + balun + GND. (d) Proposed antenna: patch + SR + balun + GND.

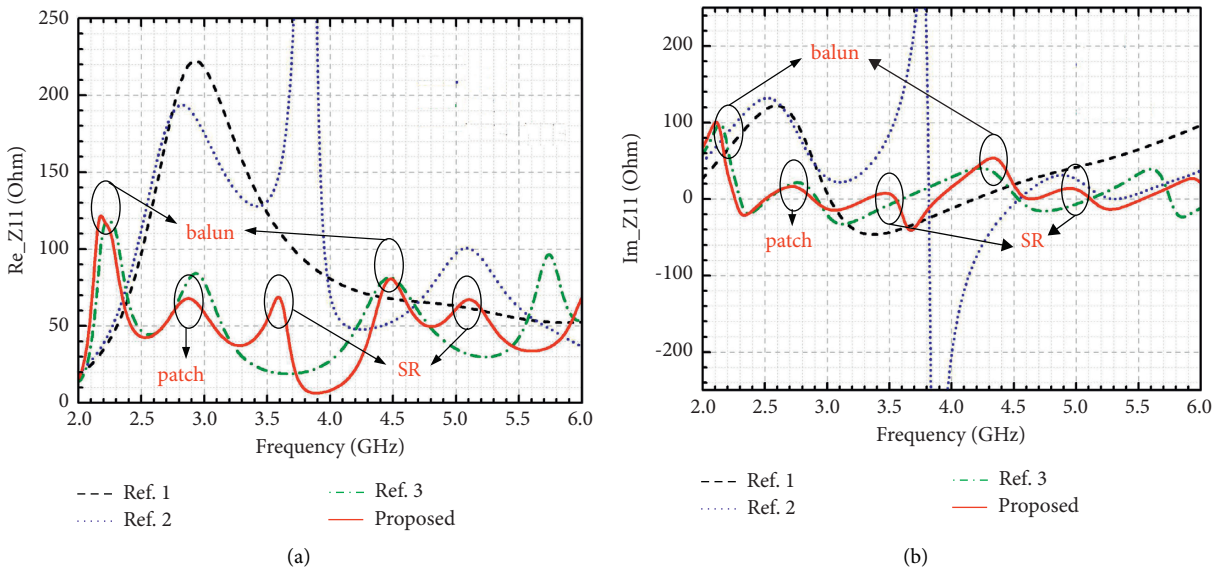


Figure 3: Input impedance of the evolution of the proposed antenna. (a) Real part and (b) imaginary part.

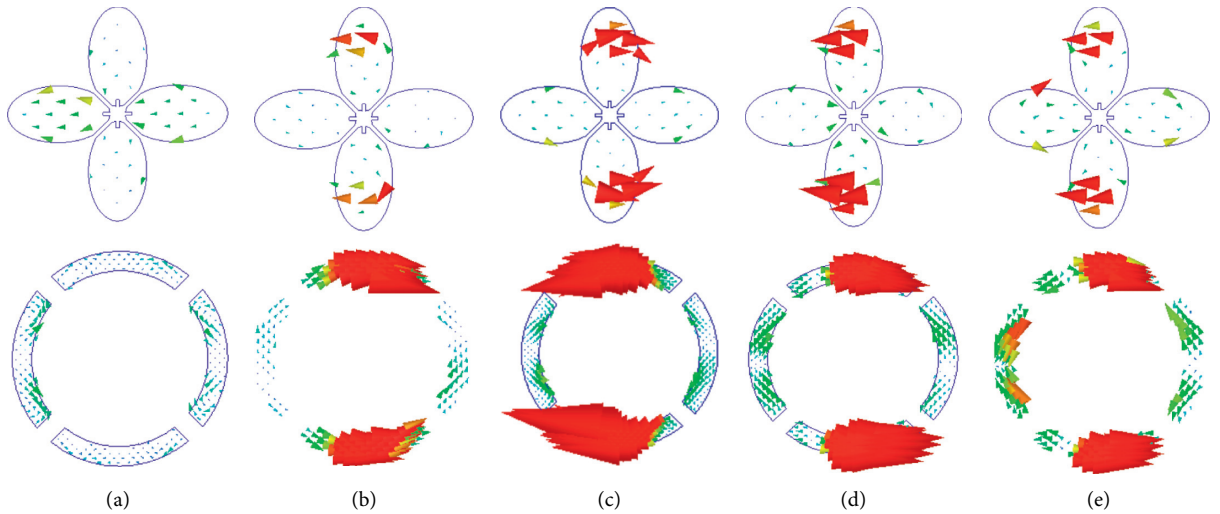


Figure 4: Simulated current distributions on the bowtie patches and SR. (a) 2.6 GHz, (b) 3.5 GHz, (c) 4.0 GHz, (d) 4.8 GHz, and (e) 5.2 GHz.

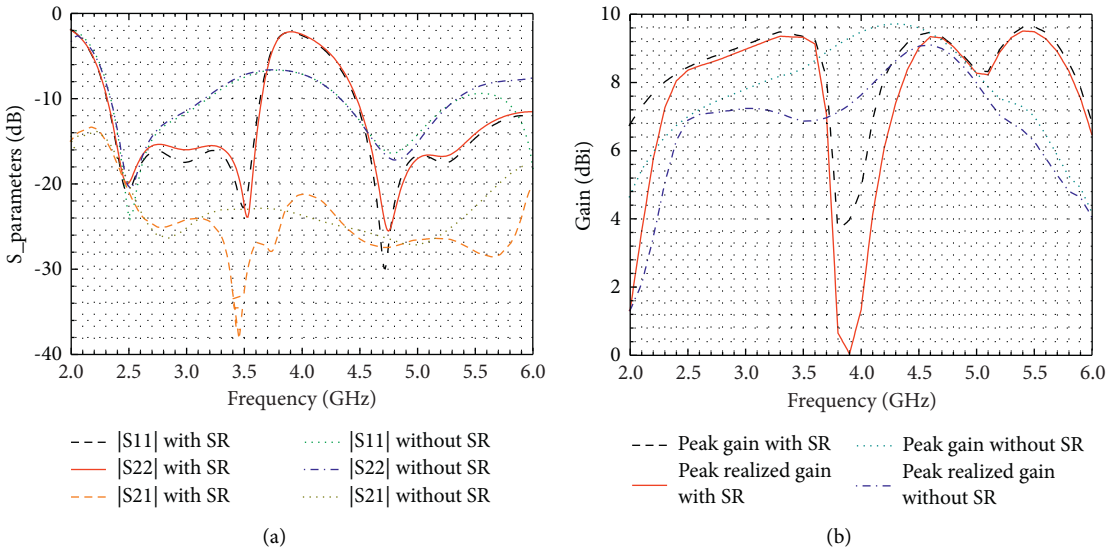


Figure 5: Comparison with and without the SR: (a) S parameters and (b) gains.

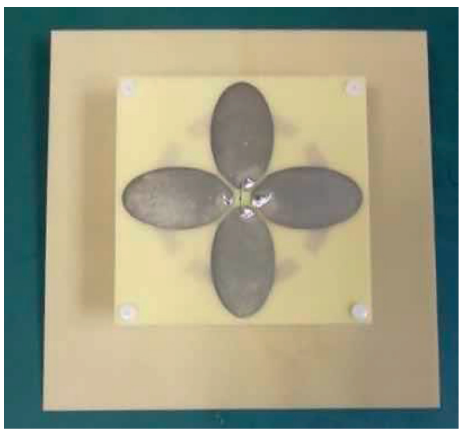

Figure 6: Photograph of the antenna prototype.

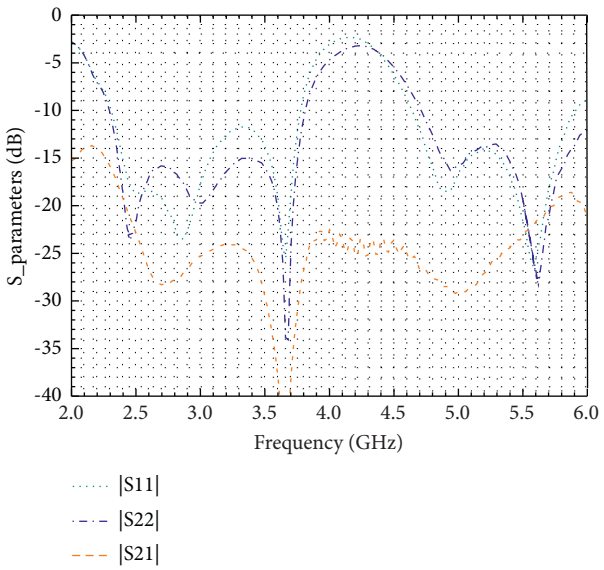


Figure 7: Measured $S$ parameters of the proposed antenna.

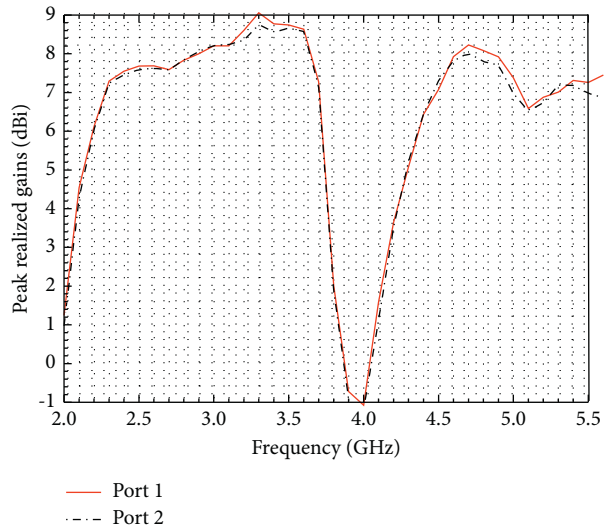


Figure 8: Measured peak realized gains of the proposed antenna.

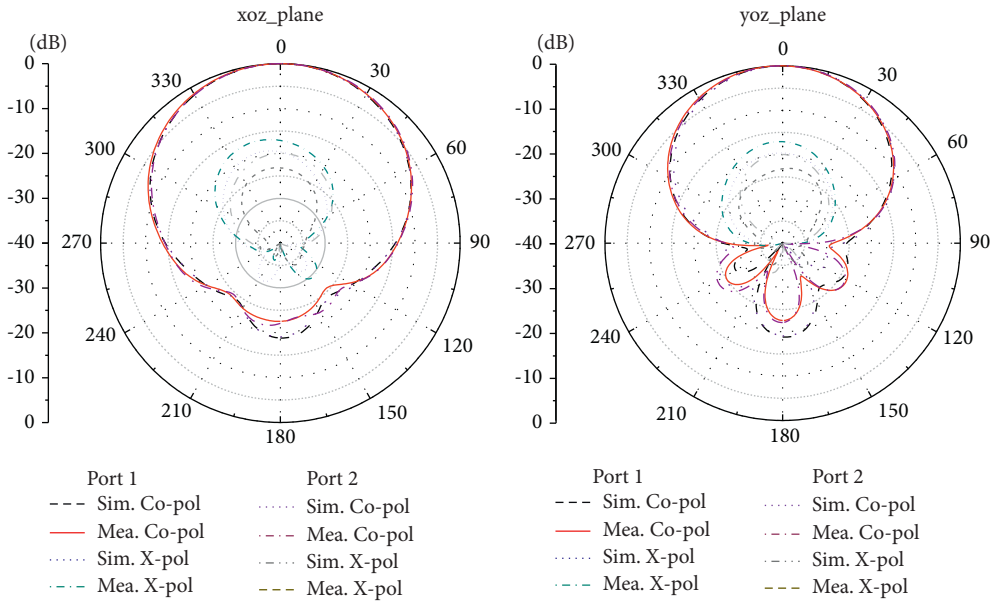


(a)

Figure 9: Continued.

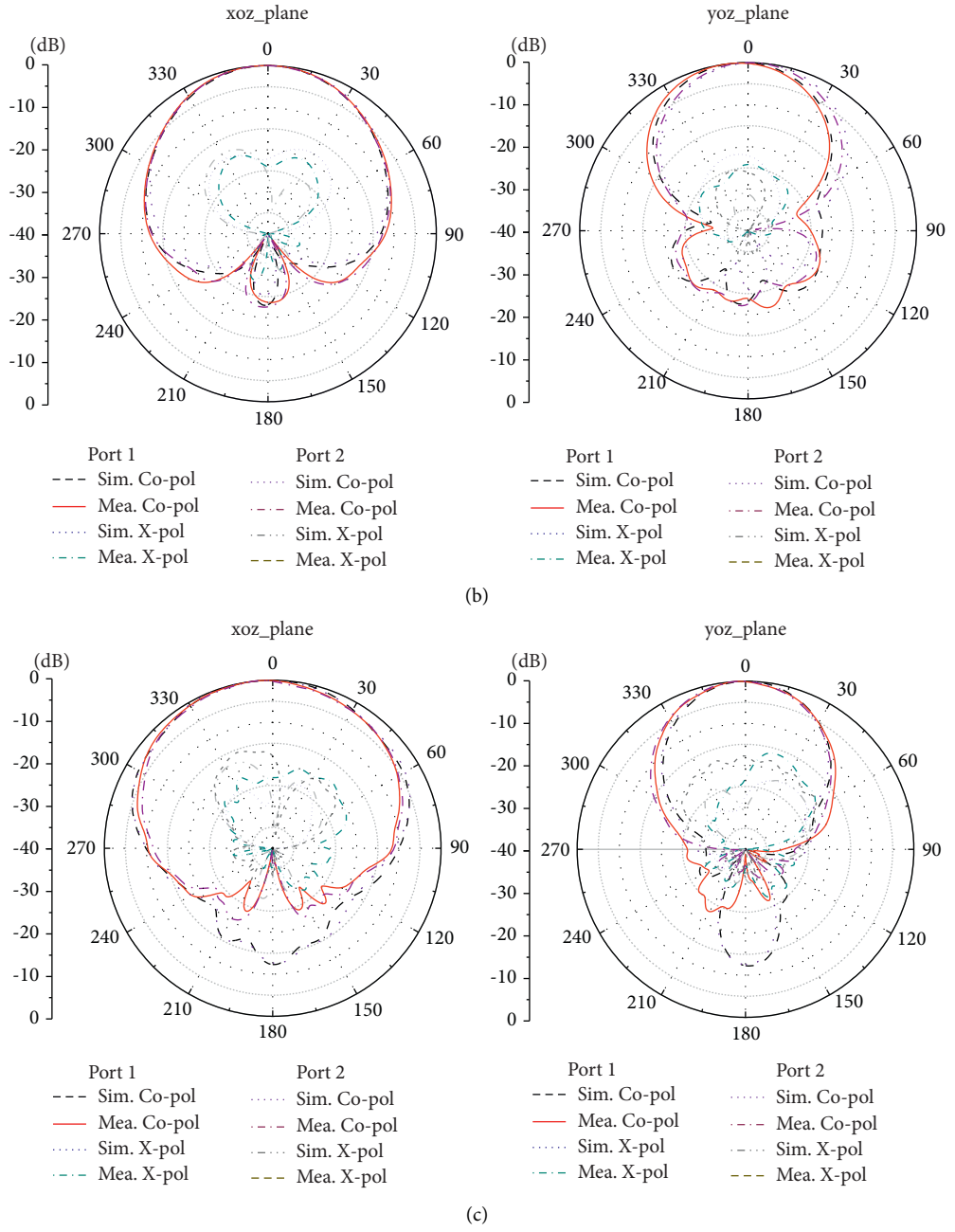


Figure 9: Simulated and measured radiation patterns of the proposed antenna at (a) 2.6 GHz, (b) 3.5 GHz, and (c) 4.8 GHz.

Table 2: Comparison with dual-band base station antennas.

| References | Size of major radiator ($\lambda_c \times \lambda_c \times \lambda_c$)* | VSWR | Bandwidth (GHz) | Isolation (dB) | Gain (dBi) |
|---|---|---|---|---|---|
| [13] | $0.97 \times 0.97 \times 0.10$ | <2.0 | 0.81–0.96 (17%) & 1.69–2.24 (28%) | >26 | $8.8 \pm 0.6/9.9 \pm 0.7$ |
| [14] | $0.35 \times 0.35 \times 0.18$ | <1.5 | 1.68–2.30 (31%) & 2.51–2.68 (7%) | >25 | $7.4 \pm 0.6/7.3 \pm 0.5$ |
| [15] | $0.50 \times 0.50 \times 0.24$ | <2.0 | 2.40–2.48 (3%) & 5.15–5.85 (13%) | >30 | $8.4 \pm 0.2/9.0 \pm 1.0$ |
| [16] | $0.63 \times 0.63 \times 0.14$ | <2.0 | 0.69–0.96 (33%) & 3.50–4.90 (33%) | >30 | $8.9 \pm 0.5/8.2 \pm 0.8$ |
| [17] | $0.30 \times 0.30 \times 0.13$ | <2.0 | 2.40–2.65 (10%) & 5.00–6.40 (25%) | >27 | $7.8 \pm 0.1/9.7 \pm 0.4$ |
| [18] | $0.48 \times 0.48 \times 0.09$ | <2.0 | 3.30–3.70 (11%) & 4.70–5.00 (6%) | >40 | $8.0 \pm 0.3/10 \pm 0.5$ |
| [19] | $0.34 \times 0.34 \times 0.27$ | <1.5 | 1.71–2.69 (45%) & 3.35–3.60 (7%) | >35 | $8.1 \pm 0.4/6.6 \pm 0.5$ |
| This work | $0.41 \times 0.41 \times 0.13$ | <2.0 | 2.31–3.77 (48%) & 4.71–5.89 (22%) | >23 | $8.2 \pm 0.7/8.1 \pm 0.6$ |

*The electric sizes are at the lowest operating frequency point.

## 4. Conclusions

In this paper, a dual-band base station antenna with an SR is presented for sub-6 GHz communications. Both the bandwidth and radiation performance are improved by two additional resonances induced at the presence of an SR. The proposed antenna can cover the three frequency bands of 2515–2675 MHz, 3400–3600 MHz, and 4800–5000 MHz.

## Data Availability

The data used to support the findings of this study are included within the article.

## Conflicts of Interest

The authors declare that there are no conflicts of interest regarding the publication of this paper.

## Acknowledgments

This work was supported in part by the National Key Research and Development Program of China (no. 2018YFB1802100), in part by the National Natural Science Foundation of China (nos. 61701120 and 61974035), and in part by the Guangdong Provincial Key Project of Science and Technology (no. 2018B010115001).

## References

[1] Y. Yuan and L. Zhu, "Application scenarios and enabling technologies of 5G," *China Communn*, vol. 11, pp. 69–79, 2014.

[2] K. F. Kin-Fai Tong, K. M. Kwai-Man Luk, K. F. Kai-Fong Lee, and R. Q. Lee, "A broad-band U-slot rectangular patch antenna on a microwave substrate," *IEEE Transactions on Antennas and Propagation*, vol. 48, no. 6, pp. 954–960, 2000.

[3] Z. Tang, J. Liu, Y.-M. Cai, J. Wang, and Y. Yin, "A wideband differentially fed dual-polarized stacked patch antenna with tuned slot excitations," *IEEE Transactions on Antennas and Propagation*, vol. 66, no. 4, pp. 2055–2060, 2018.

[4] L. Wang, K. w. Chen, Q. Huang et al., "Wideband circularly polarized cross-dipole antenna with folded ground plane," *IET Microwaves, Antennas & Propagation*, vol. 15, no. 5, pp. 451–456, 2021.

[5] L. Wu, R. Li, Y. Qin, and Y. Cui, "Bandwidth-enhanced broadband dual-polarized antennas for 2G/3G/4G and IMT services," *IEEE Antennas and Wireless Propagation Letters*, vol. 17, no. 9, pp. 1702–1706, 2018.

[6] J. Zhang and Z. Shen, "Dual-band shared-aperture UHF/UWB RFID reader antenna of circular polarization," *IEEE Transactions on Antennas and Propagation*, vol. 66, no. 8, pp. 3886–3893, 2018.

[7] K. Wang, X. Liang, W. Zhu et al., "A dual-wideband dual-polarized aperture-shared patch antenna with high isolation," *IEEE Antennas and Wireless Propagation Letters*, vol. 17, no. 5, pp. 735–738, 2018.

[8] B. Wang, C. Zhu, C. Liao, W. Luo, B. Yin, and P. Wang, "Broadband dual-polarized dipole antenna for LTE/5G base station applications," *Electromagnetics*, vol. 40, no. 1, pp. 13–22, 2020.

[9] Q. Hua, Y. Huang, A. Alieldin, C. Song, T. Jia, and X. Zhu, "A dual-band dual-polarized base station antenna using a novel feeding structure for 5G communications," *IEEE Access*, p. 1, 2020.

[10] H. Zhang, S. Yang, S. Xiao, Y. Chen, and S. Qu, "Low-profile, lightweight, ultra-wideband tightly coupled dipole arrays loaded with split rings," *IEEE Transactions on Antennas and Propagation*, vol. 67, no. 6, pp. 4257–4262, 2019.

[11] C. Weng Chew, "A broad-band annular-ring microstrip antenna," *IEEE Transactions on Antennas and Propagation*, vol. 30, no. 5, pp. 918–922, 1982.

[12] V. A. Fedotov, M. Rose, S. L. Prosvirnin, N. Papasimakis, and N. I. Zheludev, "Sharp trapped-mode resonances in planar metamaterials with a broken structural symmetry," *Physical Review Letters*, vol. 99, p. 147401, 2007.

[13] Y. Wang and Z. Du, "Dual-polarized dual-band microstrip antenna with similar-shaped radiation pattern," *IEEE Transactions on Antennas and Propagation*, vol. 63, no. 12, pp. 5923–5928, 2015.

[14] H. Huang, Y. Liu, and S. Gong, "A broadband dual-polarized base station antenna with anti-interference capability," *IEEE Antennas and Wireless Propagation Letters*, vol. 16, pp. 613–616, 2017.

[15] J.-S. Row and Y.-J. Huang, "Dual-band dual-polarized antenna for WLAN applications," *Microwave and Optical Technology Letters*, vol. 60, no. 1, pp. 260–265, 2018.

[16] Y. Chen, J. Zhao, and S. Yang, "A novel stacked antenna configuration and its applications in dual-band shared-aperture base station antenna array designs," *IEEE Transactions on Antennas and Propagation*, vol. 67, no. 12, pp. 7234–7241, 2019.

[17] Y. Zhang, Y. Zhang, D. Li, K. Liu, and Y. Fan, "Dual-polarized band-notched antenna without extra circuit for 2.4/5 GHz WLAN applications," *IEEE Access*, vol. 7, pp. 84890–84896, 2019.

[18] B. Feng, L. Li, J.-C. Cheng, and C.-Y.-D. Sim, "A dual-band dual-polarized stacked microstrip antenna with high-isolation and band-notch characteristics for 5G microcell communications," *IEEE Transactions on Antennas and Propagation*, vol. 67, no. 7, pp. 4506–4516, 2019.

[19] S. Fu, Z. Cao, X. Quan, and C. Xu, "A broadband dual-polarized notched-band Antenna for 2/3/4/5G base station," *IEEE Antennas and Wireless Propagation Letters*, vol. 19, no. 1, pp. 69–73, 2020.

[20] J. Zhang and Z. Shen, "Compact and high-gain UHF/UWB RFID reader antenna," *IEEE Transactions on Antennas and Propagation*, vol. 65, no. 10, pp. 5002–5010, 2017.

[21] K.-Z. Hu, M.-C. Tang, M. Li, and R. W. Ziolkowski, "Compact, low-profile, bandwidth-enhanced substrate integrated waveguide filtenna," *IEEE Antennas and Wireless Propagation Letters*, vol. 17, no. 8, pp. 1552–1556, 2018.